

HIGH TIME RESOLUTION GAMMA-RAY STUDIES OF CYGNUS X-1

W.T. Bridgman, M.D. Leising, DD Clayton

Department of Physics & Astronomy, Clemson University, Clemson, SC 29634-1911

M. Strickman, J.D. Kurfess, W.W. Johnson, R.L. Krizer,

RA Koeger, J.E. Groe

EO. Hulbert Center for Space Research

National Research Laboratory, Mil. Code 450, Washington, DC 20375-5320

G.V. Jug

Universities Space Research Associates

Washington, DC 20375-5320

DA Gabdulsky, WR Preece, MP Umer

Department of Physics & Astronomy, Northwestern University, Evanston, IL 60208

ABSTRACT

We report results of our studies of light time resolution data on Cygnus X-1 collected by the OSSE instrument in several observations from June, 1991 to June, 1993. Rate samples were collected in several energy bands with a time resolution of 4 milliseconds. Using Fast Fourier Transform and auto-correlation functions, we have searched these OSSE data on various timescales for evidence of flares and other time structures, both periodicities and overlapping shots. We describe these searches, present the results, and compare them with previous observations at lower energies.

INTRODUCTION

Cygnus X-1 is an X-ray and γ -ray source which varies on timescales from milliseconds to months (Rothschild et al. 1977; Sutherland, Wasskopf & Kahn 1978; Friedarsky, Terrell & Holt 1983; Friend & Giannelli 1986; Ing, Morey & Watson 1990). The millisecond variability combined with mass estimates provide compelling arguments that the power source for this object is an accretion disk surrounding a stellar mass black hole. The OSSE instrument has monitored Cygnus X-1 using its high time resolution mode on several occasions. For some observations, the detectors were operated in their regular 'chopping' mode, switching between source and background pointings every two minutes. For other observations, one or more detectors were set to stare at the source the entire time it was above the horizon. Table I summarizes these observations on which we have completed preliminary analyses.

DATA ANALYSIS

In this report, the data are collected in batches of 131.072 seconds with 4 millisecond time resolution. Each batch is then detrended by subtracting a best-fit second-order polynomial to remove effects of the South Atlantic Anomaly (SAA) and the slowly varying background rate due to geomagnetic rigidity. A Hanning filter is applied to reduce the rippling effects of data truncation and enhance the appearance of line features in the spectrum. We perform the Fast Fourier Transform (FFT) and compute the power density spectrum (PS) from the square

of the absolute value. The data-set size and resolution translates to a frequency space range of zero to 125 Hz and a resolution of $125/16384 = 0.0073$ Hz. The HFS of each batch are then added together (called incoherent summing since the phase information from the HFS is lost) in the hope that features due to random noise will tend to cancel out while real features due to the source variability will be enhanced. Some results of this process are illustrated in Figure 1.

Table I OSSE Viewing periods with RATE data for Cygnus X-1

Detector - hours On-Target	Low Energy Window	Average cts/sec	High Energy Window	Average cts/sec	Average Flux ^b	Comments
VP 002: 91/157 - 91/166 (June 6-15, 1991)						
8.49 hr	40-190 keV	299.5	190-780 keV	170.9	8.68×10^{-2}	VP 002a
22.58 hr	33-132 keV	259.4	132-630 keV	121.1	7.92×10^{-2}	
14.81 hr	33-132 keV	245.4	132-630 keV	118.5		staring
VP 203: 92/343 - 92/344 (December 8-9, 1992)						
14.47 hr	88-140 keV	105.5	140-414 keV	137.6	6.42×10^{-2}	staring
VP 223: 93/151 - 93/154 (May 31-June 3, 1993)						
18.44 hr	40-70 keV	83.7	70-169 keV	65.7	6.19×10^{-2}	

^a Includes background flux

^b Flux in 45-140 keV band, photons / s / cm²

The detrending process creates the low power near zero Hz. The error bars represent the standard deviation of the mean. We see no significant features like the quasi-periodic oscillations (QPO) reported by some observers at energies below 70 keV (Vrtilek et al. 1992; Agolini et al. 1992; Kavadiou et al. 1992, 1993). Even the small features in the summed spectra are generally not consistent among the multiple detectors, a good example being the ‘feature’ at ≈ 0.07 Hz in VP203, which is clear in only two of the four detectors used for the observation. In addition, the appearance of features varies with the batch size chosen for the HFS, lending additional support to the notion that they are the result of random fluctuations. However, the general appearance of the spectra themselves varies considerably from one viewing period to the next and may be related to the variability in total flux from Cygnus X-1.

The autocorrelation function (ACF) is calculated in 6144 second batches and then summed. The functional form for the chosen autocorrelation function is

$$C_{yy}(u) = \frac{1}{N-u} \sum_{i=0}^{N-u-1} (y_i - \bar{y})(y_{i+u} - \bar{y})$$

(Eckson & Orosz 1968) which generates good results for finite-sized data sets. The ACF, if they show any structure at all, reveal approximately exponentially decaying profiles. Like the HFS, they vary considerably from one viewing period to the next.

THE SINE EXPONENTIAL MODEL

One of the popular models for the time variability of Cygnus X-1 is the shot noise model which assumes the signal is composed of ‘shots’ which turn on suddenly, then slowly decay

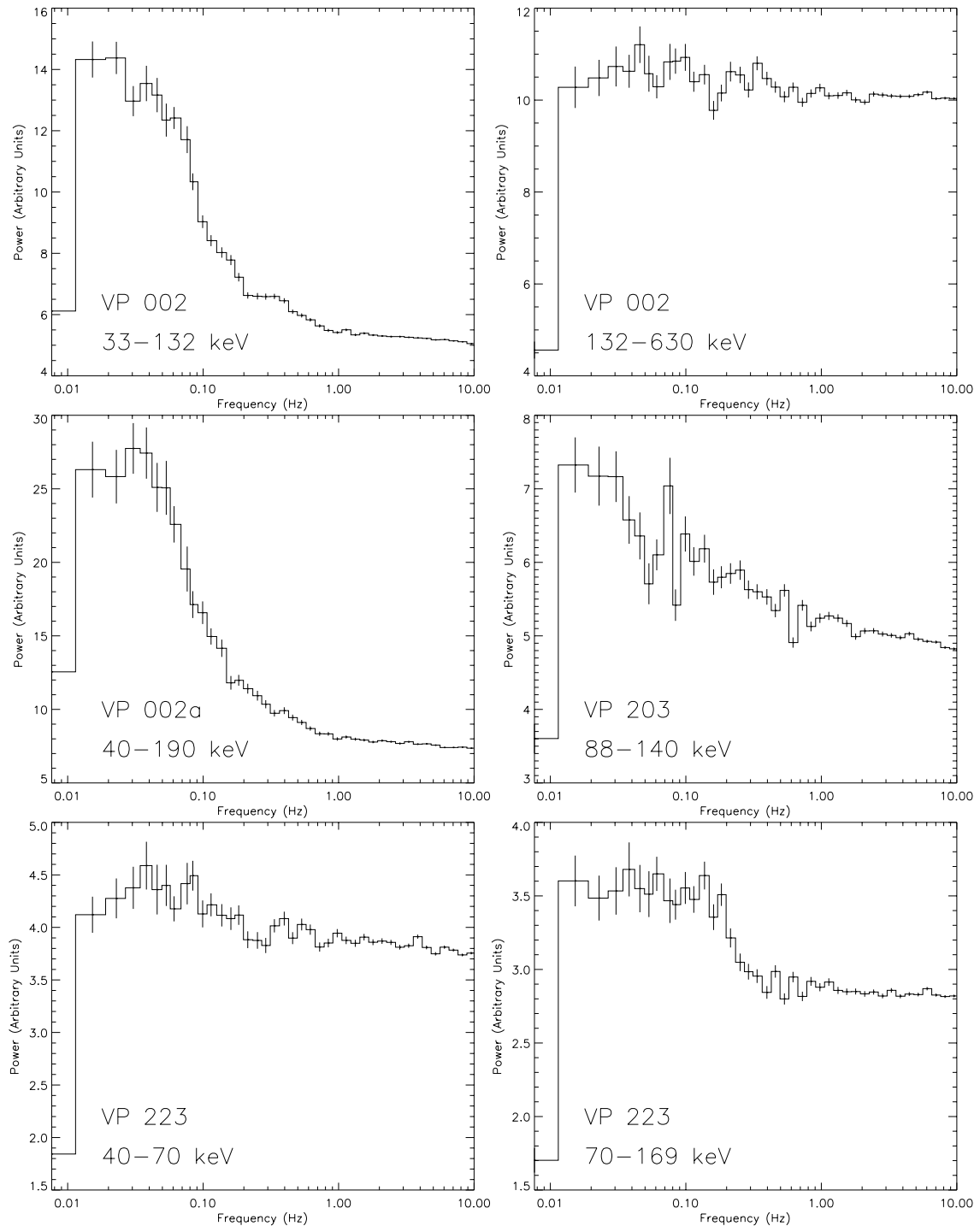


Figure 1: Some of the averaged Power Density Spectra for Viewing Periods described in Table I. The results are averaged over the detectors and rebinned on a logarithmic scale. Note that the y-axis minimum is not zero. The spectra vary considerably from one viewing period to the next.

(Sutherland et al. 1978; Melis et al. 1984; Lochner 1999). A common shot model is the simple exponential shot which has the functional form

$$f(t) = \begin{cases} 0, & t < 0 \\ e^{-t/\tau}, & t \geq 0 \end{cases}$$

where τ is a characteristic decay time for the shot.

RESULTS

The single shot model assumes the signal is generated by a random superposition of shots of constant amplitude and time constant plus a constant noise level. The double shot model assumes the signal is composed of noise and two uncorrelated shots, each with its own amplitude and time constant. Tables II and III show the results of fitting these models for observations with some time structure.

Table II Model Fits: Single Shot Model

Viewing Period	Energy (keV)	AIS			HTF		
		τ (ns)	χ^2/df	df	τ (ns)	χ^2/df	df
002a	40-190	957.7 $\pm^{5.2}_{32.7}$	1.128	1497	1461 $\pm^{8.7}_{60.5}$	1.062	297
20B	80-140	30.2 $\pm^{2.2}_{2.3}$	1.028	247	56.3 $\pm^{0.3}_{7.4}$	1.9876	297
20B	140-414	107.8 $\pm^{2.6}_{17.5}$	1.0341	247	79.8 $\pm^{4.1}_{74.7}$	1.802	297

Table III Model Fits: Double Shot Model

Viewing Period	Energy (keV)	AIS			HTF		
		τ_1 (ns)	χ^2/df	df	τ_1 (ns)	χ^2/df	df
		τ_2 (ns)			τ_2 (ns)		
002a	40-190	1380.6 $\pm^{8.5}_{62.3}$	0.723	2138	7 $\pm^{0.1}_{18.0}$	0.8786	
		25.8 $\pm^{4.4}_{2.5}$	145		311.5 $\pm^{6.7}_{61.0}$		295
20B	80-140	137.9 $\pm^{6.9}_{4.1}$	0.9121	7616	2 $\pm^{9.2}_{24.6}$	1.9348	
		18.1 $\pm^{4.4}_{3.3}$	245		421.5 $\pm^{5.8}_{39.6}$		295
20B	140-414	152.5 $\pm^{3.8}_{5.6}$	0.959	7633	9 $\pm^{0.8}_{48.8}$	1.8061	
		2.5 $\pm^{4.4}_{1.3}$	245		695.9 $\pm^{6.2}_{39.6}$		295

The agreement of the time constants for the AIS and HTF is poor, but it does seem that the values for the HTF are consistently greater than those for the AIS. We see three possible explanations for this difference: 1) There are additional time structures in the G rms X1 output which appear in the HTF but not in the AIS; 2) The shots do not have a simple exponential profile; 3) The shot model paradigm is not applicable at all.

There is also considerable difference between the time constants for the single and double shot models. In fact, the primary motivation for investigating the double shot model was the appearance in many of the AIS of an apparent steep exponential drop at short lag times which merged into a much gentler exponential-like decline at longer lags. This is very apparent in the relative sizes of the two time constants for the AIS. It's also worth noting that while good fits are obtained with both the AIS and HTF in VP02a, the HTF have much poorer fits in VP20B. The shot times for VP20B are also quite different from Lochner (1999) who

obtained shot times from 0.82 to 1.46 seconds at energies below 60 keV and Stlerland, et al. (1978) with times from 0.35 to 0.67 seconds between 1.8 and 8.6 keV.

The HF and AIS at energies below ≈ 10 keV show some time structure, but the higher energies look like random noise. Since we know that Cygnus X1 generates photons in this higher energy range, one wonders if the region generating them has any detectable time structure. Alternatively, these photons might be Compton up-scattered from the lower energies over such large distances that the oscillations are washed out. To wash out say 0.10 Hz oscillations the scattering path length would have to be on the order of 10 cm. If we assume the X-ray source is a 10 solar mass black hole, this distance corresponds to $\approx 50,000$ Schwarzschild radii, which is far larger than the high temperature ($T \approx 10^6 K$) of our current black hole accretion disk models. The model of Maccarone & McClintock (1993) for Cygnus X1 indicate that the innermost region of the accretion disk should be optically thick. This region could therefore act as a direct source for these photons and provide sufficient scattering to remove any temporal signatures from the lower energy photons. Alternatively, their model exhibits considerable structural changes for the inner disk with changes in the disk viscosity and accretion rate. These structural changes or the structures themselves may be the source of the radical variations in the temporal signatures displayed in separate viewing periods.

This research was supported by NASA DRS 1087C Work at Clemson supported by Grant No. N0014-1-G15 from the Naval Research Laboratory.

REFERENCES

- Agolli, L., White, NE & Stella, L., IAU Circular 550 (1992).
- Edelson, L. & Orosz, R. 1998, Programming and Analysis for Digital Time Series Data (The Stock and Watson Information Center) p. 130
- Fried, D. & Cassioli, J. 1986, AJ, 93, 292
- Kouveliotou, C., Finger, M., Fishman, G., Meegan, C., Wilson, R., & Paciesas, W. 1992, IAU Circular 556 (1992).
- Kouveliotou, C., Finger, M., Fishman, G., Meegan, C., Wilson, R., Paciesas, W., Maritani, T. & van Paradijs, J. 1993, APC Conference Proceedings 280, p. 319
- Ling, J., Morey, W. & Watson, W. 1990, 21st ICRC, 197.
- Ichner, J. 1989, PhD Thesis, University of Maryland.
- Melis, J., Wal, K., Helder, R., Bram, E., Yatis, D., Clith, T. & Friedman, H. 1984, AJ, 278, 288.
- Maccarone, F. & McClintock, R. 1993, AJ, 411, 797.
- Piedlarsky, W., Errel, J. & Hilt, S. 1983, AJ, 270, 233.
- Rothschild, R., Bild, E., Hilt, S. & Serleitsos, P. 1977, AJ, 213, 818.
- Stlerland, P., Wasskopf, M. & Kahn, S. 1978, AJ, 219, 1029.
- Voklinin, A., Suyaev, R., Chrazov, E., Gilfanov, M., Bilek, J., Doris, M., Laurent, P. & Reves, J.P., IAU Circular 556 (1992).